JOURNAL OF COMPUTATIONAL PHYSICS 114, 77–84 (1994)

A Method to Suppress the Finite-Grid Instability in Plasma Simulations*

J. U. BRACKBILL

Los Alamos National Laboratory, Los Alamos, New Mexico

AND

GIOVANNI LAPENTA

Politecnico di Torino, Torino, Italy

Received October 19, 1993

A technique for suppressing the finite-grid instability in plasma simulation by jiggling the computation mesh is revisited. Linear dispersion theory suggests a reduction in growth rate of 50% when the mesh is randomly jiggled. With an implicit method, a large time step, and a grid with variable spacing, a nearly complete absence of the instability is observed. Because of its simplicity and low cost, it is suggested the method can be used routinely with variable zoning or adaptive grids to suppress the finite-grid instability.

INTRODUCTION

For more than 20 years, it has been known that particle-in-cell (PIC) plasma simulations are unstable due to aliasing errors [1, 2]. This instability, called the finite-grid instability, also occurs in PIC fluid models [3] and is due to undersampling of the particle data in the calculation of interaction among the particles on the grid. The instability can cause rapid, unphysical heating of the plasma and, consequently, large errors in energy conservation.

The instability is a very serious problem for PIC, yet there are many successful simulations with no evidence of its appearance. Knowledgeable researchers have chosen problem parameters to avoid the instability, they have used higher-order interpolation, and they have smoothed the data and interlaced or jiggled grids to reduce its growth rate [4, 5]. Further, they have been quick to recognize and discard those calculations where the instability has caused large errors. In implicit methods, where the time step is very large compared with the plasma frequency, the growth rate for the instability is less, but the instability still imposes a weak constraint on the minimum time step that can be used [6].

The finite-grid instability becomes more than an annoyance when one considers multiple-length scale problems. For example, one may have a collisionless shock with very strong gradients embedded in a more-or-less uniform plasma. Clearly, in such cases there is an advantage to concentrating grid points in the region of strong gradients using variable zoning. On a nonuniform grid, it can be impossible to use a single time step everywhere in the domain and satisfy the condition for stability. Precisely this situation is illustrated by the variable grid calculation of a slow shock shown below. To address the problem of the finite-grid instability on a variable grid, we re-examine a technique suggested by Chen [4] for suppressing the instability, a "jiggled" grid. Here we report very positive results with a jiggled grid. The differences between our technique and that described by Chen [4] are explained, a stability analysis is presented, and comparisons between slow shock calculations with and without jiggling the mesh are presented.

FINITE-GRID INSTABILITY ON AN IRREGULAR MESH

We consider the finite-grid instability on a mesh with nodes located at

$$x_j' = j\,\Delta x + \delta x_j, \qquad j \in [1, J], \tag{1}$$

where δx_j can be different for every j. For simplicity, we consider a continuous number density, $n(x)$, and a mollified number density $\bar{n}(x)$, calculated by convolving $n(x)$ with a "shape" function, $S(x)$,

$$\bar{n}(x) = \int dx'\, n(x')\, S(x - x'). \tag{2}$$

* The U.S. Government's right to retain a nonexclusive royalty-free license in and to the copyright covering this paper, for governmental purposes, is acknowledged.

0021-9991/94 $6.00

We assume S is positive with bounded support and that it satisfies the integrability condition. The Fourier transform of $\bar{n}(x)$ is given by

$$\bar{N}(k) = N(k)\, S(k), \tag{3}$$

where $N(k)$ and $S(k)$ are the Fourier transforms of $n(x)$ and $S(x)$, respectively.

The finite-grid instability is caused by aliases. Aliases arise when we evaluate the inverse transform at the mesh points,

$$\bar{n}(x_j') = \int_{-\infty}^{\infty} \frac{dk}{2\pi} \bar{N}(k)\, e^{ikx_j'}. \tag{4}$$

To evaluate $\bar{n}$, first define k_l by

$$k_l = \bar{k} + lk_g, \qquad \bar{k} \in \left[\frac{-\pi}{\Delta x}, \frac{\pi}{\Delta x}\right], \tag{5}$$

where $k_g = 2\pi/\Delta x$ is the first harmonic of the shortest wavelength mode resolved by a uniform mesh with spacing Δx, and $\bar{k}$ is the principal wave number. It follows that

$$e^{ik_l j\,\Delta x} = e^{i\bar{k}j\,\Delta x}. \tag{6}$$

With these definitions, the inverse transform can be written

$$\bar{n}(x_j') = \int_{-\pi/\Delta x}^{\pi/\Delta x} \frac{d\bar{k}}{2\pi} e^{i\bar{k}j\,\Delta x} \sum_{l=-\infty}^{\infty} \bar{N}(k_l)\, e^{ik_l \delta x_j}. \tag{7}$$

In this inverse transform, each alias, $-\infty \leqslant l \leqslant \infty$, is multiplied by a complex phase factor due to the irregular spacing.

One can construct an ensemble of meshes, each with a different set of displacements, δx_j, according to a probability distribution $P(\delta x)$. The average of the results with many sets of displacements is given by

$$\langle \bar{n}_j \rangle = \int_{-\infty}^{\infty} P(\delta x_j)\, \bar{n}_j(\delta x_j)\, d(\delta x_j). \tag{8}$$

A particularly interesting probability function from the viewpoint of computation is one that gives a uniform distribution on the interval $-\Delta \leqslant \delta \leqslant \Delta$. The result of an ensemble average of Eq. (7) with a uniform probability distribution is

$$\langle \bar{n}_j \rangle = \int_{-\pi/\Delta x}^{\pi/\Delta x} \frac{d\bar{k}}{2\pi} e^{i\bar{k}j\,\Delta x} \sum_{l=-\infty}^{\infty} \bar{N}(k_l)\, \mathrm{dif}\left(k_l \frac{\Delta}{2}\right), \tag{9}$$

where the diffraction function is defined by

$$\mathrm{dif}\left(k_l \frac{\Delta}{2}\right) = \sin\left(k_l \frac{\Delta}{2}\right) \Big/ \left(k_l \frac{\Delta}{2}\right). \tag{10}$$

When one jiggles the mesh randomly, the average result is to multiply each alias by the diffraction function. Next, the effect of this factor is examined by evaluating the linear dispersion for various values of Δ.

One notes one small difference between the jiggling described by Chen *et al.* [4] and the algorithm described above. Chen proposed displacing each grid point the same distance so that the displaced grid also had uniform spacing. The jiggling described above will result in nonuniform spacing. Thus, it requires appropriate differencing for nonuniform meshes, but it also extends the approach to aperiodic domains.

LINEAR DISPERSION OF THE VLASOV-POISSON SYSTEM

Consider the solution of the linearized Vlasov–Poisson equations in one dimension, written

$$\frac{\partial f_1}{\partial t} + v \frac{\partial f_1}{\partial x} + a_1 \frac{\partial f_0}{\partial v} = 0, \tag{11}$$

$$a_1 = \frac{q}{m} E_1, \tag{12}$$

$$\frac{\partial E_1}{\partial x} = 4\pi q n_1, \tag{13}$$

and

$$n_1 = \int_{-\infty}^{\infty} f_1\, dv; \qquad n_0 = \int f_0\, dv. \tag{14}$$

The distribution function, $f(x, v)$ gives the number of particles in an element of phase-space (dx, dv) at (x, v). The zero-order distribution is uniform and stationary:

$$\frac{\partial f_0}{\partial x} = \frac{\partial f_0}{\partial t} = 0. \tag{15}$$

Consider a time-centered, implicit discretization of Eq. (11) written

$$\frac{f_1^{n+1} - f_1^n}{\Delta t} + v \frac{\partial f_1^{n+1/2}}{\partial x} + a_1^{n+1/2} \frac{\partial f_0}{\partial v} = 0, \tag{16}$$

where

$$f^{n+1} = f(t + \Delta t), \qquad f^n = f(t). \tag{17}$$

(This implicit formulation is approximated by the implicit-moment and direct-implicit methods [7, 8].) If one assumes the time and space dependence,

$$f_1(x, v, t) = e^{-i(\omega t - kx)} F_{k,\omega}(v), \tag{18}$$

one can write Eq. (16) as

$$-i(\Omega - kv)\, F_{k,\omega} + A_{k,\omega} \frac{\partial f_0}{\partial v} = 0, \tag{19}$$

where Ω is given by

$$\Omega \frac{\Delta t}{2} = \tan\left(\frac{\omega\, \Delta t}{2}\right). \tag{20}$$

and $A_{k,\omega}$ is the Fourier transform of the acceleration,

$$A_{k,\omega} = \frac{q}{m} S(k) \frac{4\pi q}{ik} \sum_l N(k_l)\, S(k_l)\, \mathrm{dif}\left(k_l \frac{\Delta}{2}\right). \tag{21}$$

One can integrate Eq. (19) over v and factor N_k to derive the dispersion relation,

$$0 = 1 + \omega_L^2 \sum_l \frac{S^2(k_l)\, \mathrm{dif}(k_l \Delta/2)}{n_0 k_l} \int \frac{(\partial f_0/\partial v)\, dv}{(\Omega - k_l v)}, \tag{22}$$

where

$$\omega_L^2 = \frac{4\pi n_0 q^2}{m}. \tag{23}$$

As noted by many authors, the additional resonances, contributed by the aliases, $\pm l \in [1, \infty]$, are the cause of the finite-grid instability.

A particularly simple case is that of a cold beam moving with velocity v_B through a fixed, charge neutralizing background,

$$f_0 = \delta(v - v_B). \tag{24}$$

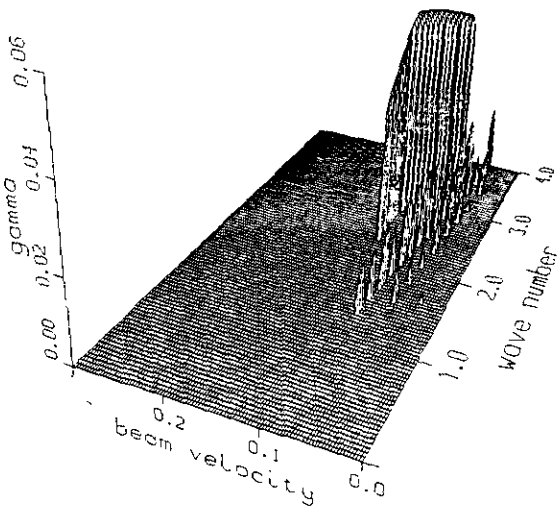

FIGURE 2

The dispersion relation, Eq. (22), reduces to

$$0 = \Omega^2 - \sum_{l=-\infty}^{\infty} \omega_L^2 S^2(k_l)\, \mathrm{dif}\left(\frac{k_l \Delta}{2}\right)\left(1 \Big/ \left(1 - \frac{k_l v_B}{\Omega}\right)^2\right). \tag{25}$$

The dispersion is evaluated numerically with linear interpolation, for which $S(k)$ is given by

$$S(k) = \left(\mathrm{dif}\left(k \frac{\Delta x}{2}\right)\right)^2, \tag{26}$$

and the results are shown in Figs. 1–3. For reference the imaginary part of the frequency for a case with $\omega_L\, \Delta t = 0.2$ and without jiggling is shown in Fig. 1. For beam velocities less than $\sim 0.2 \omega_L\, \Delta x$, there are exponentially growing

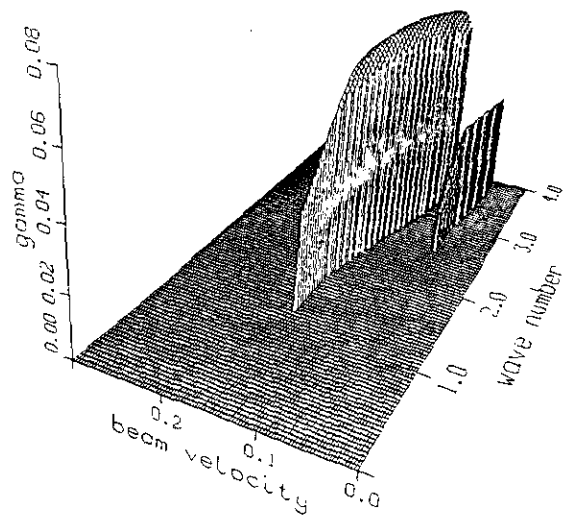

FIGURE 1

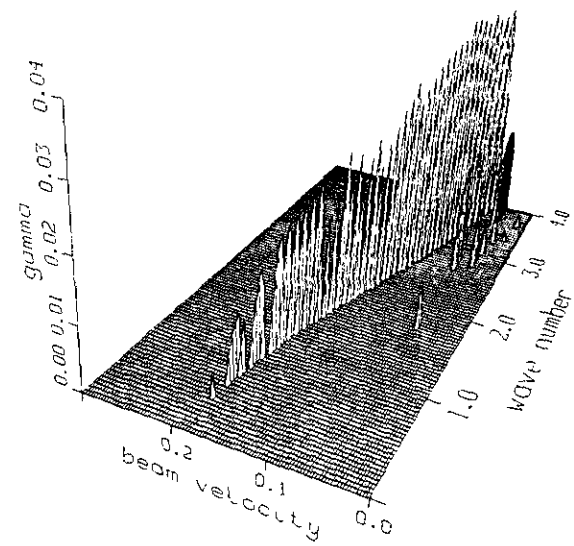

FIGURE 3

solutions with growth times, $\omega_L t \sim 12$–16. When the mesh is jiggled with $\Delta = 0.5$, Fig. 2, the region of instability is restricted to a smaller range of velocities, $v_b < 0.15\omega_L \Delta x$, to shorter wavelengths, and to longer growth times, $\omega_L t \sim 16$–25. When the mesh is jiggled with $\Delta = 1$, Fig. 3, the instability is restricted to a narrow band of wave numbers for a given velocity. One notes that one can evaluate Eq. (25) with the contributions of one or two aliases included, $-n \leqslant l \leqslant n$, where $n = 1, 2$, etc. Such experiments indicate that the band of greatest instability can be associated with the contribution from the first alias, $l = \pm 1$. A comparison of Figs. 1 and 3 suggests that jiggling can suppress the first alias completely.

COLD BEAM: NUMERICAL EXPERIMENTS

Nonlinear solutions of the cold-beam problem are generated with CELEST1D, an implicit-moment simulation code for plasmas in one dimension [9]. Only electrostatic interactions are included. The calculation is similar to that reported by Chen *et al.*, with 32 cells, 64 particles per cell, and a cold beam with $v_B = 0.32\omega_L \Delta x$. However, a larger time step is used, $\omega_L \Delta t = 1$, but it is not so large that there should be significant differences from the earlier results.

A plot of the beam is shown in Fig. 4 for $\omega_L t = 400$. The finite grid instability has caused a large amplitude modulation of the particle velocity and, as shown in Fig. 5, a large increase in the thermal energy of the beam, $\langle (v - v_B)^2 \rangle$. The maximum value is nearly 5% of the initial beam energy.

We next jiggle the mesh. Instead of jiggling the mesh and averaging the results for a single time step, a random displacement is imposed once each time step. When there are high correlations from time step to time step, time averaging over several time steps is equivalent to ensemble averaging in a single time step. Time and ensemble averages are only approximately equivalent, and the approximation is less likely to be accurate in the beam case, where the instability growth time is only several time steps.

With jiggling and $\Delta = 0.8$, the results are shown in Figs. 6 and 7. There is some modulation in the beam velocity, Fig. 6, but much smaller than without jiggling. There is also some increase in the thermal energy, Fig. 7, but this time it is to a maximum that is less than 1% of the initial beam energy. Abe estimates that the energy increase due to the instability should scale as the square of the growth rate

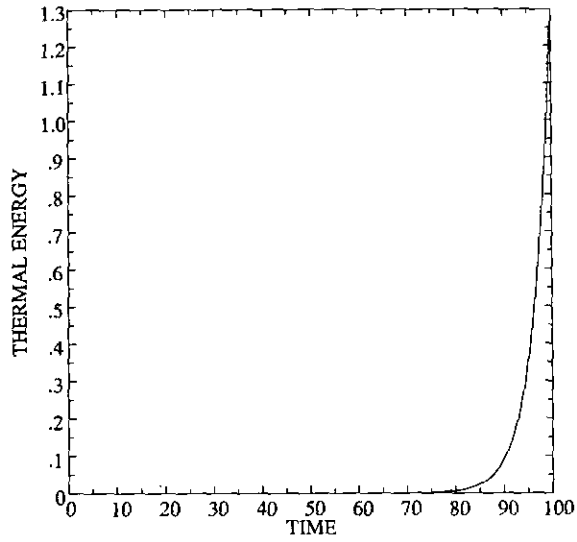

FIGURE 5

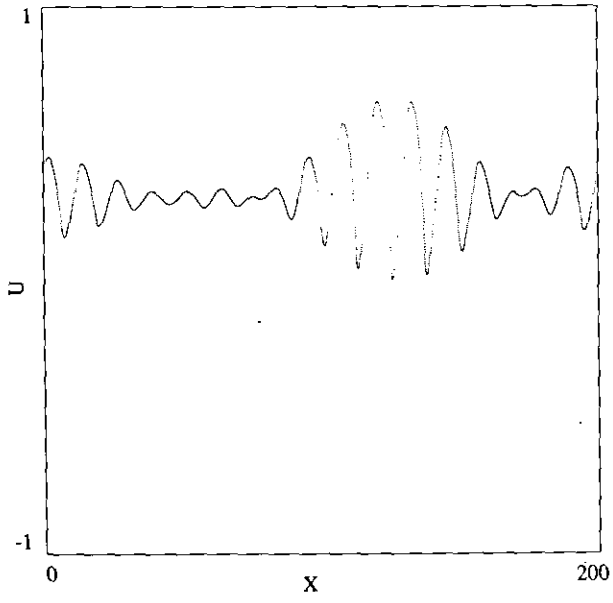

FIGURE 4

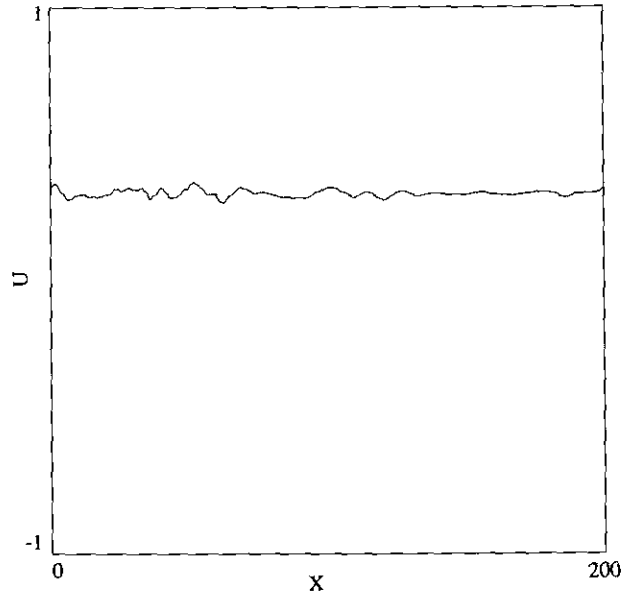

FIGURE 6

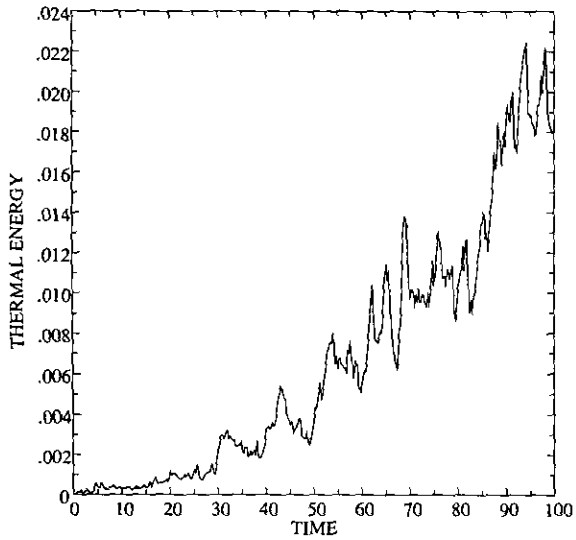

FIGURE 7

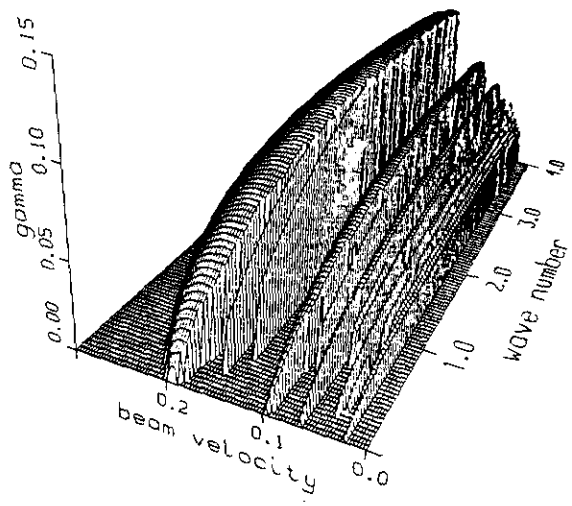

FIGURE 9

[10]. Thus, it appears that jiggling has halved the growth rate of the instability, which is consistent with the linear dispersion results above.

To summarize, these results seem entirely consistent with those presented earlier by Chen *et al.* [4] and Birdsall and Maron [5]. One difference not shown is that the decrease in growth rate with δx_j, selected independently for each j, is greater than with $\delta x_j = \text{const}$, $j \in [1, N]$. As observed earlier, jiggling reduces the growth rate but does not suppress the instability.

FINITE TIME STEPS

Several studies have investigated the effect of large time steps on the plasma dispersion, e.g., Brackbill and Forslund [7]. The effect of discretization in time is to limit the maximum representable frequency to the Nyquist frequency, $\omega_N = \pi/\Delta t$. Thus, as Δt increases, the value of the plasma frequency decreases with increasing Δt. As shown earlier, so does the growth rate of the finite grid instability. As a result, implicit calculations with $\omega_L \Delta t \gg 1$ and $\lambda_D/\Delta x \ll 1$, where λ_D is the Debye length, $\lambda_D = v_{\text{thermal}}/\omega_L$, are stable. For example, in calculations of the collisionless slow shock, stable solutions are obtained with $\lambda_D/\Delta x \cong 2.5 \times 10^{-4}$ and $\omega_L \Delta t = 250$ ($v_{\text{thermal}} \Delta t/\Delta x = 7 \times 10^{-2}$).

Results with $\omega_L \Delta t = 0.2$ and nearest-grid-point (NGP) interpolation, Fig. 8, can be compared with those for $\omega_L \Delta t = 4$, Fig. 9. The increase in the time step halves the maximum growth rate. When $\omega_L \Delta t = 4$ and the mesh is jiggled with $\Delta = 1$, Fig. 10, the maximum growth rate is halved again. Thus, the stabilizing effect of large time steps and jiggling is additive.

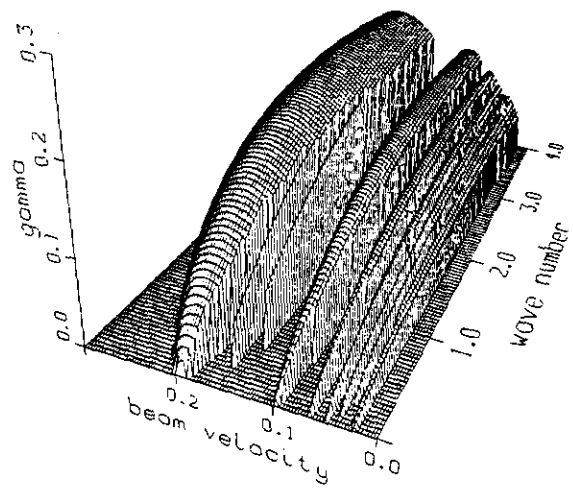

FIGURE 8

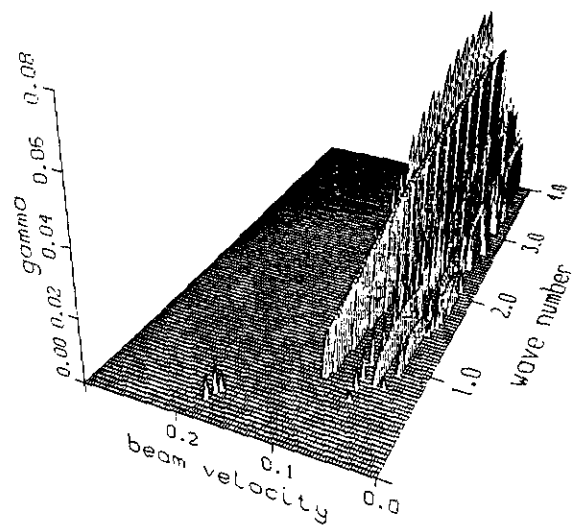

FIGURE 10

COLLISIONLESS SLOW-SHOCK

In the slow-shock calculations, a magnetized plasma is injected at the left boundary and reflects at the right boundary. The upstream flow conditions and the downstream boundary conditions produce a switch-off slow-shock that propagates upstream with a constant velocity. Behind the shock, there is a circularly polarized wave, which has been called a trailing magnetic wave (TMW) [11]. There are several papers on the slow-shock, including one on a calculation with kinetic electrons as is considered here [12].

Because of the absence of interesting features in the upstream regions, it seems reasonable that an adaptive grid with small zones only in the shock would be more efficient computationally. Efficiency is not an academic issue, even in one dimension, because the simulations have required as much as 4 h of CRAY computer time to perform.

When a calculation is performed on a uniform grid with 400 cells, $\lambda_D/\Delta x = 2.5 \times 10^{-4}$, $\omega_{Li}\,\Delta t = 50$, and 256 electron and 64 ion particles per cell initially, there is no instability. However, there is an instability when an adaptive grid is used. With 260 cells, and a mesh varying in size from $4 \times 10^3 \lambda_D \leqslant \Delta \leqslant 1.28 \times 10^5 \lambda_D$, the grid spacing is plotted in Fig. 11. The stack plot, Fig. 12, plots profiles of the z-component of the magnetic field at intervals of $\omega_{Li} t = 100$ from $t = 0$ to $\omega_{Li}\,\Delta t = 5000$, where ω_{Le}/ω_{Li}, the ratio of electron to ion plasma frequency is 5. In the stack plot, one can identify the steady progression of the shock to the left and the TMW behind. One can also see very large amplitude waves upstream. These have no physical cause and are evidence of the growth of the finite-grid instability. In the hodogram, Fig. 13, in which By is plotted against Bz as a point moves from left to right, the TMW is identifiable as the spiral portion of the curve. The large amplitude waves upstream appear chaotic, with random changes in phase from point to point.

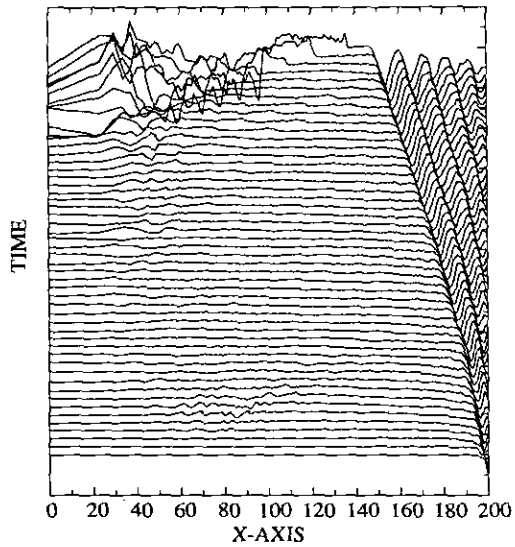

FIGURE 12

Using the mesh shown in Fig. 11, with jiggling, produces the results shown in Figs. 14 and 15. The hodogram in Fig. 15 is especially useful in judging the amplitude of the upstream waves, because the amplitude of the TMW is the same as in Fig. 13. The amplitude of the upstream waves is negligible with jiggling. In this case, which is typical of the problems one would like to do, jiggling is effective in reducing the effect of finite-grid instability and results in a 30% reduction in the cost of the calculation.

Another aspect of the effect of jiggling is shown in Figs. 16–17. In Fig. 16, the total kinetic energy without jiggling

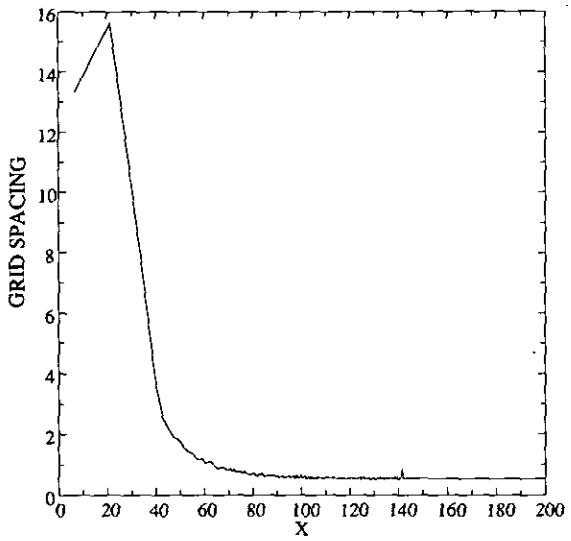

FIGURE 11

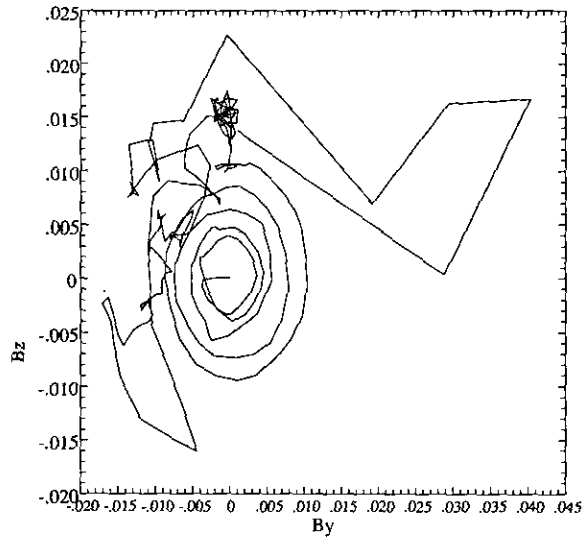

FIGURE 13

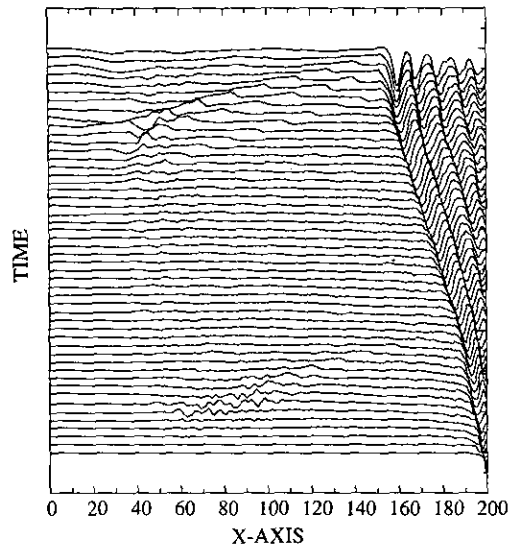

FIGURE 14

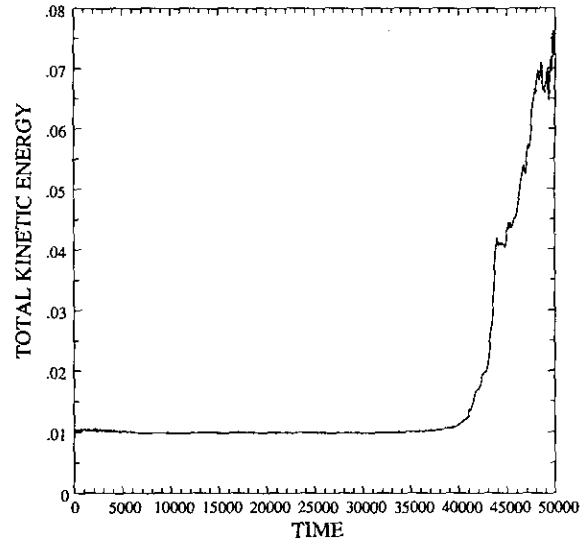

FIGURE 16

grows rapidly to eight times its initial value from $\omega_{pe}t = 4 \times 10^4$ until the end of the calculation. There are pauses, but the growth appears to occur in a single episode. In Fig. 17, the total kinetic energy with jiggling increases by 40% between $\omega_{pe}t = 3.8 \times 10^4$ and $\omega_{pe}t = 4.3 \times 10^4$. Thereafter, the energy increases at an average rate that appears to be linear in time. Evidently, the instability is not eliminated by jiggling, but its growth rate and saturation amplitude are reduced substantially.

The grid, Fig. 11, has very large zones near the left boundary. There $\Delta = 0.25$ and, on the time step shown, there is a large variation in zone size from cell to cell. In the vicinity of the shock, $x = 140c/\omega_{Li}$, the grid is not jiggled at all. The mesh spacing is already sufficiently small so that the instability does not occur and there is no need to do anything further. One can imagine the decision to jiggle or not could be based on the value of $\lambda_D/\Delta x$, but the critical value depends upon the time step and the distribution function as expressed by a dispersion relation similar to Eq. (22). Thus, the estimate of the critical value would itself require a numerical solution of the dispersion equation.

The calculation shown in Figs. 11–15 requires the solution of the electromagnetic equations. As is well known, the solution of these equations requires that one store a previous value of the vector potential at each grid point [9]. When the mesh is jiggled, these stored values must be interpolated to the new grid. In the case shown in Figs. 14–15, the interpolation used is a cubic spline routine [13]. In two

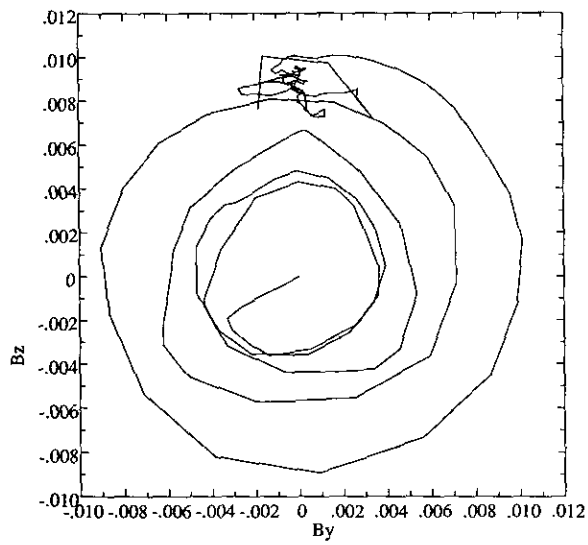

FIGURE 15

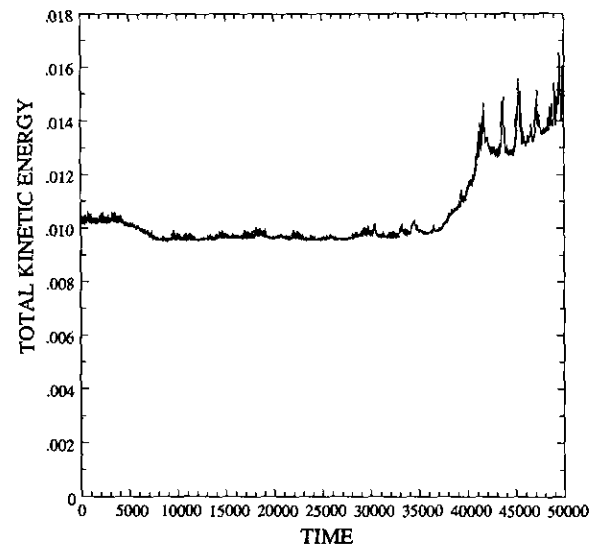

FIGURE 17

or three dimensions, this is not possible to use. Calculations with linear interpolation were observed to have enough numerical diffusion to eliminate the TMW, so that whatever technique is used should be $O(\Delta x^3)$. Of course, interpolation introduces diffusion each time step with diffusivity $O(\Delta x^n/\Delta t)$. For convergence as $\Delta t \to 0$, Δx must also decrease so that the diffusivity remains bounded.

CONCLUSION

A technique for suppressing the finite-grid instability suggested by Chen *et al.* is revisited [4]. It is found that jiggling the mesh is very effective in suppressing the instability in collisionless shock calculations on a grid with wide variations in cell size.

That it should be successful in reducing the growth rate is suggested by dispersion analysis, but it is not explained by it. There is no theory for the instability in electromagnetic plasma simulation, and so it is not known whether there is an electromagnetic branch to the instability. Evidently, there is coupling to the magnetic field because of the large amplitude variations in the field. Other diagnostics, not shown, indicate the principal effect of the instability is plasma heating just as in the electrostatic case and that coupling to the magnetic field occurs as a side effect of the change in plasma properties.

Finally, a key assumption of the technique is the equivalence of ensemble and time averaging. Numerical experiments suggest that, if there is sufficient correlation in the particle data over several time steps, the technique works as the analysis predicts. Furthermore, the cost of jiggling the grid, if one is already using a variable-spaced grid, is negligible.

ACKNOWLEDGMENT

The authors gratefully acknowledge the support of the U.S. Department of Energy, Office of Fusion Energy, for this research.

REFERENCES

1. E. L. Lindman, *J. Comput. Phys.* **5**, 13 (1970).
2. A. B. Langdon, *J. Comput. Phys.* **6**, 247 (1970).
3. J. U. Brackbill, *J. Comput. Phys.* **75**, 469 (1988).
4. L. Chen, A. B. Langdon, and C. K. Birdsall, *J. Comput. Phys.* **14**, 200 (1974).
5. C. K. Birdsall and N. Maron, *J. Comput. Phys.* **36**, 1 (1980).
6. J. U. Brackbill and D. W. Forslund, *J. Comput. Phys.* **46**, 271 (1982).
7. J. U. Brackbill and D. W. Forslund, in *Multiple Time Scales*, edited by J. U. Brackbill and B. I. Cohen (Academic Press, Orlando, 1985), p. 271.
8. A. B. Langdon and D. C. Barnes, in *Multiple Time Scales*, edited by J. U. Brackbill and B. I. Cohen (Academic Press, Orlando, 1985), p. 335.
9. H. X. Vu and J. U. Brackbill, *Comput. Phys. Commun.* **69**, 253 (1992).
10. H. Abe, J. Miyamoto, and R. Itatani, *J. Comput. Phys.* **19**, 134 (1975).
11. F. V. Coroniti, *J. Geophys. Res.* **11**, 261 (1971).
12. J. U. Brackbill and H. X. Vu, *Geophys. Res. Lett.*, submitted.
13. H. Akima, *J. Assoc. Comput. Mach.* **17**, 589 (1970).